

## Chondroitin Sulfate Extracted from Ascidian Tunic Inhibits Phorbol Ester-Induced Expression of Inflammatory Factors VCAM-1 and COX-2 by Blocking NF- $\kappa$ B Activation in Mouse Skin

CHENG-XIONG XU,<sup>†,‡</sup> HUA JIN,<sup>†,∇</sup> YOUN-SUN CHUNG,<sup>‡</sup> JI-YOUNG SHIN,<sup>‡</sup>  
 KEE-HO LEE,<sup>#</sup> GEORGE R. BECK, JR.,<sup>⊥</sup> GRACE N. PALMOS,<sup>||</sup>  
 BYEONG-DAE CHOI,<sup>\*,||</sup> AND MYUNG-HAING CHO<sup>\*,‡,§,○</sup>

Laboratory of Toxicology, College of Veterinary Medicine, and Nano Systems Institute, National Core Research Center, Seoul National University, Seoul 151-742, Korea; Laboratory of Molecular Oncology, Korea Institute of Radiological and Medical Sciences, Seoul 139-240, Korea; Division of Endocrinology, Metabolism and Lipids, Emory University School of Medicine, Atlanta, Georgia 30322; Division of Marine Life Science/Institute of Marine Industry, Gyeongsang National University, Tongyoung 650-160, Korea; Center for Developmental Pharmacology and Toxicology, Seattle Children's Hospital Research Institute, Seattle, Washington 98101; and National Institute of Toxicological Research, Seoul 122-704, Korea

Inflammatory factors are known to play a key role in promoting tumorigenesis; therefore, it is a promising strategy to inhibit the inflammation for cancer prevention. The current study was performed to investigate the potential effects of chondroitin sulfate (CS) extracted from ascidian tunic on the expression of inflammatory factors induced by treatment with 12-*O*-tetradecanoylphorbol-13-acetate (TPA) and to elucidate the underlying molecular mechanism of CS action in mouse skin inflammation. TPA was topically applied to the shaven backs of ICR mice with or without CS (1 or 2 mg) for 4 h. The results demonstrated that CS suppressed TPA-induced edema and reduced the expression of cyclooxygenase-2, vascular cell adhesion molecule-1, and Akt signaling in mouse skin. These studies suggest that CS from ascidian tunic may be developed as an effective natural anti-inflammatory agent.

**KEYWORDS:** Ascidian tunic; chondroitin sulfate; VCAM-1; COX-2; NF- $\kappa$ B; Akt

### INTRODUCTION

Inflammation is considered to be an important component of tumorigenesis, although the underlying mechanisms remain largely unknown (1). Interestingly, benign tumor cells induce inflammatory response in the host and collaborate in establishing the tumor through a process called desmoplasia (2). Essentially, all of the elements that constitute the inflammatory response participate in the host reaction, which could, therefore, have an atrophic purpose for tumor cells (3).

Nuclear factor  $\kappa$ B (NF- $\kappa$ B) is a ubiquitous and well-characterized protein responsible for the regulation of complex

phenomena, with a pivotal role in controlling cell signaling in the body under certain conditions. Among other functions, NF- $\kappa$ B controls the expression of genes encoding the pro-inflammatory cytokines, for example, interleukin-1 (IL-1), tumor necrosis factor- $\alpha$  (TNF- $\alpha$ ), chemokines such as IL-8, macrophage inflammatory protein-1 $\alpha$  (MIP-1 $\alpha$ ), and monocyte chemoattractant protein-1 (MCP-1), adhesion molecules such as vascular cell adhesion molecule (VCAM), and inducible enzymes such as cyclooxygenase-2 (COX-2), all of which play critical roles in controlling inflammatory processes (4). Because NF- $\kappa$ B represents an important and very attractive therapeutic target for treating many inflammatory diseases, much attention has focused on the identification of compounds that selectively interfere with this pathway (5). Recently, many natural substances have been evaluated as possible inhibitors of the NF- $\kappa$ B pathway such as caffeic acid phenethyl ester, capsaicin, and resveratrol (5).

Diverse cellular signaling components consisting of serine/threonine kinases and redox-regulated transcription factors are involved in the regulation of COX-2 and VCAM-1 expression in response to pro-inflammatory stimuli (6, 7). Topical application of a tumor promoter, 12-*O*-tetradecanoylphorbol-13-acetate

\* Corresponding authors [(M.-H.C.) telephone +82-2-880-1276, fax +82-2-873-1268, e-mail mchotox@snu.ac.kr; (B.-D.C.) telephone +82-55-640-3173, fax +82-55-640-3173, e-mail bdchoi@gnu.ac.kr].

<sup>†</sup> These authors contributed equally to this work.

<sup>‡</sup> Laboratory of Toxicology, Seoul National University.

<sup>∇</sup> Seattle Children's Hospital Research Institute.

<sup>#</sup> Korea Institute of Radiological and Medical Sciences.

<sup>⊥</sup> Emory University School of Medicine.

<sup>||</sup> Gyeongsang National University.

<sup>§</sup> Nano Systems Institute, Seoul National University.

<sup>○</sup> National Institute of Toxicological Research.

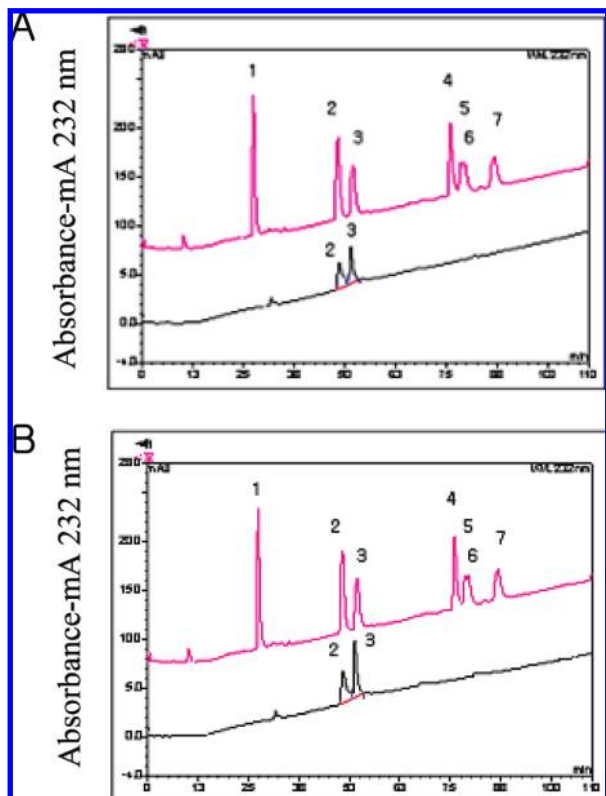


**Figure 1.** Strong anion-exchange HPLC analysis of the disaccharides formed by specific lyases on the ascidian glycosaminoglycans. A mixture of chondroitin standard disaccharides and the disaccharides formed by the exhaustive action of chondroitinase ABC (A, subscript abc) and AC (B, subscript ac) on the glycans for fractions was applied to a 25 cm × 4.6 mm Phenosphere-SAX column linked to an HPLC system. The column was eluted with a linear gradient of NaCl. The eluent was monitored for UV absorbance at 232 nm. The chondroitin sulfate disaccharide standards used were as follows: peak 1, OS,  $\alpha$ - $\Delta$ UA-1  $\rightarrow$  3-GalNAc; peak 2 (CSA), 6S,  $\alpha$ - $\Delta$ UA-1  $\rightarrow$  3-GalNAc(6diSO<sub>4</sub>); peak 3 (CSC), 4S,  $\alpha$ - $\Delta$ UA-1  $\rightarrow$  3-GalNAc(4diSO<sub>4</sub>); peak 4, SD,  $\alpha$ - $\Delta$ UA(2SO<sub>4</sub>)-1  $\rightarrow$  3-GalNAc(6diSO<sub>4</sub>); peak 5, SE,  $\alpha$ - $\Delta$ UA-1  $\rightarrow$  3-GalNAc(4,6-diSO<sub>4</sub>); peak 6, SB,  $\alpha$ - $\Delta$ UA(2SO<sub>4</sub>)-1  $\rightarrow$  3-GalNAc(4diSO<sub>4</sub>); peak 7, TriS,  $\alpha$ - $\Delta$ UA(2SO<sub>4</sub>)-1  $\rightarrow$  3-GalNAc(4,6-diSO<sub>4</sub>). Please note that the upper chromatograms in **A** and **B**, respectively, represent the internal standards, whereas the lower chromatograms are generated from the CS mixture, indicating that the CS mixture contains only two fractions of peaks 2 (CSA) and 3 (CSC).

(TPA) induced COX-2 and VCAM-1 mRNA transcription and protein expression in mouse skin (8, 9). The genes of COX-2 and VCAM-1 contain several binding motifs for different transcription factors including eukaryotic transcription factor NF- $\kappa$ B (10). NF- $\kappa$ B, predominantly as a heterodimer of p65 and p50, binds to the  $\kappa$ B consensus sequence located in the COX-2 and VCAM-1 gene promoter, thereby regulating protein expressions (10, 11). In physiologic state, NF- $\kappa$ B is retained in cytosol as an inactive complex with its inhibitory protein I $\kappa$ B $\alpha$ , which blocks nuclear translocation of NF- $\kappa$ B (12). Phosphorylation of I $\kappa$ B $\alpha$  and its subsequent ubiquitination and proteasomal degradation upon inflammatory stimuli make NF- $\kappa$ B free to translocate into nucleus and bind to  $\kappa$ B regulatory elements (13). The I $\kappa$ B $\alpha$  phosphorylation is triggered by the activation of the I $\kappa$ B kinase (IKK) complex (14). Recent studies indicate that IKK $\beta$ -dependent NF- $\kappa$ B activation creates an essential link between inflammation and cancer (14, 15). Besides IKKs, several other protein kinases are also reported to regulate NF- $\kappa$ B activation. Of these upstream kinases, the role of mitogen-

**Table 1.** Disaccharide Composition of the GAGs Fraction<sup>f</sup>

peak <sup>a</sup>	disaccharide	t <sub>R</sub> <sup>b</sup> (min)	proportion of the disaccharides <sup>c</sup> (% total)	
			A <sub>abc</sub> <sup>d</sup>	A <sub>ac</sub> <sup>e</sup>
1	Di-OS	27.35	ND	ND
2	Di-6S	47.79	49.32	43.10
3	Di-4S	51.40	50.68	56.90
4	Di-S <sub>D</sub>	74.93	ND	ND
5	Di-S <sub>E</sub>	77.95	ND	ND
6	Di-S <sub>B</sub>	78.49	ND	ND
7	Di-TriS	85.66	ND	ND

<sup>a</sup> Standard peak number in order of elution; see **Figure 1**. <sup>b</sup> Retention time of the disaccharides on a Phenosphere-SAX column linked to an HPLC system. <sup>c</sup> Areas under the peaks in **Figure 1** were integrated to obtain the disaccharide composition. ND, not detected. <sup>d</sup> Ascidian fraction treated with chondroitinase ABC. <sup>e</sup> Ascidian fraction treated with chondroitinase AC. <sup>f</sup> Average peak area of peak 2 (Di-6S, CSA) is 46.21 [(49.32(A<sub>abc</sub>) + 43.10(A<sub>ac</sub>))/2]; average peak area of peak 3 (Di-4S, CSC) is 53.79 [(50.68(A<sub>abc</sub>) + 56.90(A<sub>ac</sub>))/2] in HPLC chromatogram. Together, approximate ratio between CSA and CSC is 46:54 (v/v).

activated protein kinases (MAPKs), such as p38 MAPK, in regulating NF- $\kappa$ B activation has been well-documented (16). Another serine/threonine kinase, Akt, which promotes cell survival by preventing apoptosis (17), has also been reported to regulate COX-2 expression through the NF- $\kappa$ B/I $\kappa$ B pathway (18).

Chondroitin sulfate (CS) is a glycosaminoglycan (GAG), which is naturally present in the extracellular matrix of articular cartilage (19). Recently, several studies indicated that CS played an important role in anti-inflammation and anticancer, and a few studies were performed to elucidate the underlying molecular mechanism. Legendre et al. reported that CS inhibited pro-inflammatory gene expression such as COX-2 and iNOS in chondrocytes (20); however, they did not provide detailed information of how CS suppresses the pro-inflammatory factor expression. Recently Campo et al. found that CS inhibited collagen-induced NF- $\kappa$ B activation (21). However, the precise mechanism of CS was not investigated thoroughly either. In this study, therefore, we investigated anti-inflammatory effects of CS on TPA-induced inflammation in mouse skin in vivo and explored the underlying molecular mechanism.

## MATERIALS AND METHODS

**Materials.** Ascidiens were collected from Tongyoung, South Korea. TPA, chondroitin AC lyase (EC 4.2.2.5) from *Arthrobacter aurenses*, and chondroitin ABC lyase (EC 4.2.2.4) from *Proteus vulgaris* were purchased from Sigma-Aldrich (St. Louis, MO). Standard disaccharides  $\alpha$ - $\Delta$ UA-1  $\rightarrow$  3-GalNAc,  $\alpha$ - $\Delta$ UA-1  $\rightarrow$  3-GalNAc(6diSO<sub>4</sub>),  $\alpha$ - $\Delta$ UA-1  $\rightarrow$  3-GalNAc(4diSO<sub>4</sub>),  $\alpha$ - $\Delta$ UA(2SO<sub>4</sub>)-1  $\rightarrow$  3-GalNAc(6diSO<sub>4</sub>),  $\alpha$ - $\Delta$ UA-1  $\rightarrow$  3-GalNAc(4,6-diSO<sub>4</sub>),  $\alpha$ - $\Delta$ UA(2SO<sub>4</sub>)-1  $\rightarrow$  3-GalNAc(4diSO<sub>4</sub>), and  $\alpha$ - $\Delta$ UA(2SO<sub>4</sub>)-1  $\rightarrow$  3-GalNAc(4,6-diSO<sub>4</sub>) were purchased from Seikagaku (Tokyo, Japan); DEAE-Sepharose was from GE Healthcare Bio-Sciences AB (Uppsala, Sweden); 1,9-dimethylmethylene blue was from Sigma-Aldrich. Antiphospho-Akt (Ser473) and phospho-p65 (Ser536) antibodies were purchased from Cell Signaling Technology (Beverly, MA). Primary antibodies for VCAM-1, COX-2, NF- $\kappa$ B p65, I $\kappa$ B $\alpha$ , p-I $\kappa$ B $\alpha$ , IKK $\beta$ , phospho-IKK $\beta$ , p38, phospho-p38, nucleoporin, and actin were purchased from Santa Cruz Biotechnology (Santa Cruz, CA). Monoclonal antibodies against Akt1 and phospho-Akt at Thr308 were produced using a general method described elsewhere (22). Anti-rabbit, anti-mouse, and anti-goat horseradish peroxidase-conjugated secondary antibodies were purchased from Zymed Laboratories (San Francisco, CA).

**Isolation and Characterization of GAGs.** The tunics were separated from the ascidian bodies and frozen at -40 °C until further analysis. One kilogram of tunics was extracted under pressure at 121 °C for 3 h with 0.01 M sodium phosphate buffer and concentrated in a vacuum evaporator until a Brix value of 9–10 was obtained. The extracts were

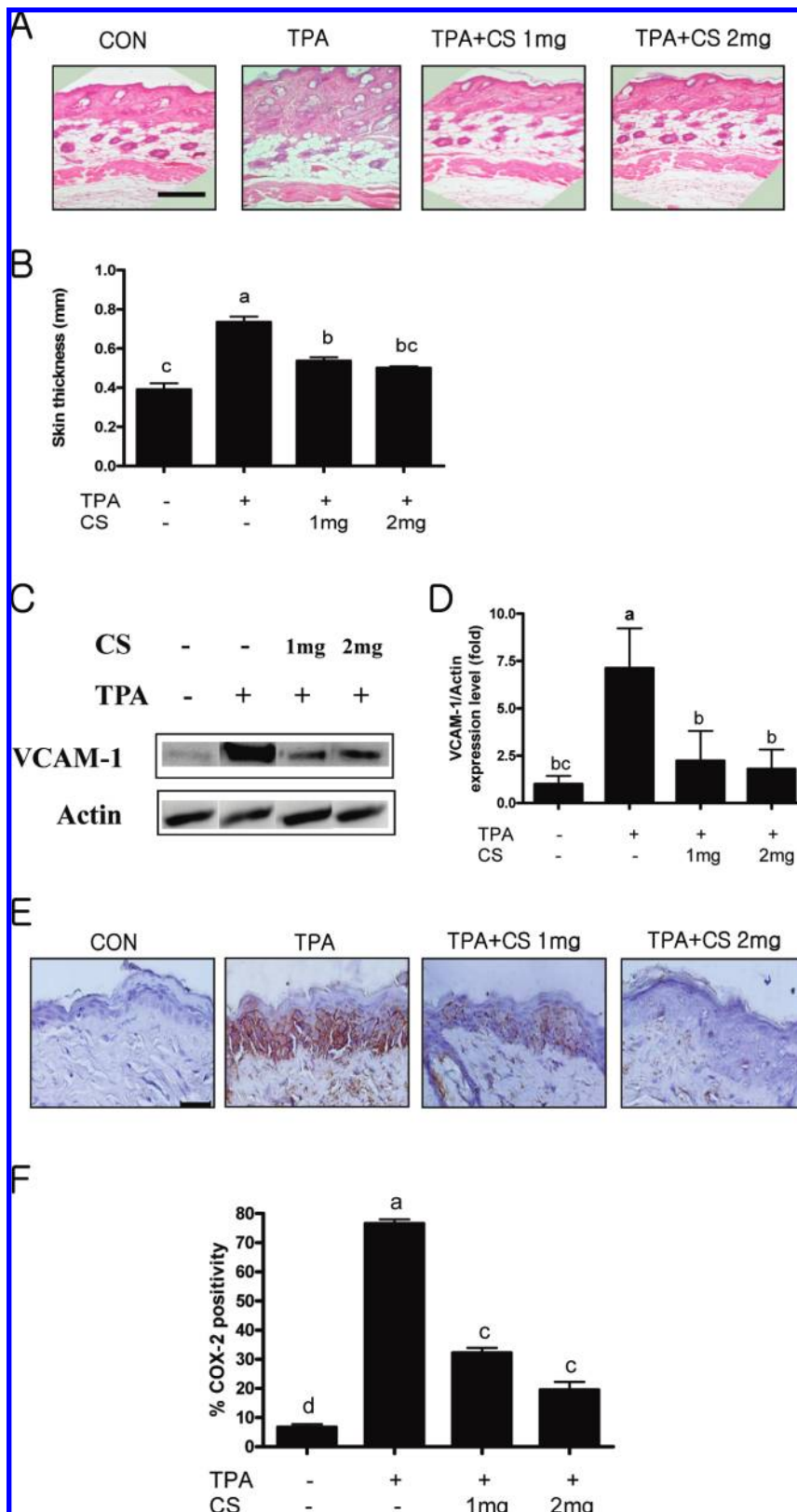


**Figure 2.** Inhibitory effects of CS on TPA-induced edema and expression of VCAM-1 and COX-2 in mouse skin. Mice were treated topically with TPA (200  $\mu$ L of 10 nmol of TPA dissolved in acetone) in the presence or absence of CS (1 or 2 mg). Control animals were treated with acetone alone. (A) Skin section was stained with hematoxylin and eosin (original magnification,  $\times 100$ ; bar, 100  $\mu$ m); (B) thickness of the skin (the thickness of the ear of each mouse was determined by averaging the values measured at five independent regions of the cross-section); (C) Western blot analysis of VCAM-1 expression in mouse skin; (D) bands of interests were further analyzed by densitometer; (E) immunohistochemical measurement of COX-2 in the mouse skin (dark brown color indicates COX-2 expression (original magnification,  $\times 200$ ; bar, 100  $\mu$ m); (F) comparison of COX-2 labeling index in the mouse skin (COX-2-positive staining was determined by counting five randomly chosen fields per section, determining the percentage of DAB-positive cells per 100 cells at  $\times 400$  magnification. Different letters (a–c) denote statistical difference ( $P < 0.05$ ). Each bar represents the mean  $\pm$  SE ( $n = 3$ ). CON, control; TPA, TPA-treated group; TPA + CS, TPA-treated mice in the presence of CS (1 or 2 mg).

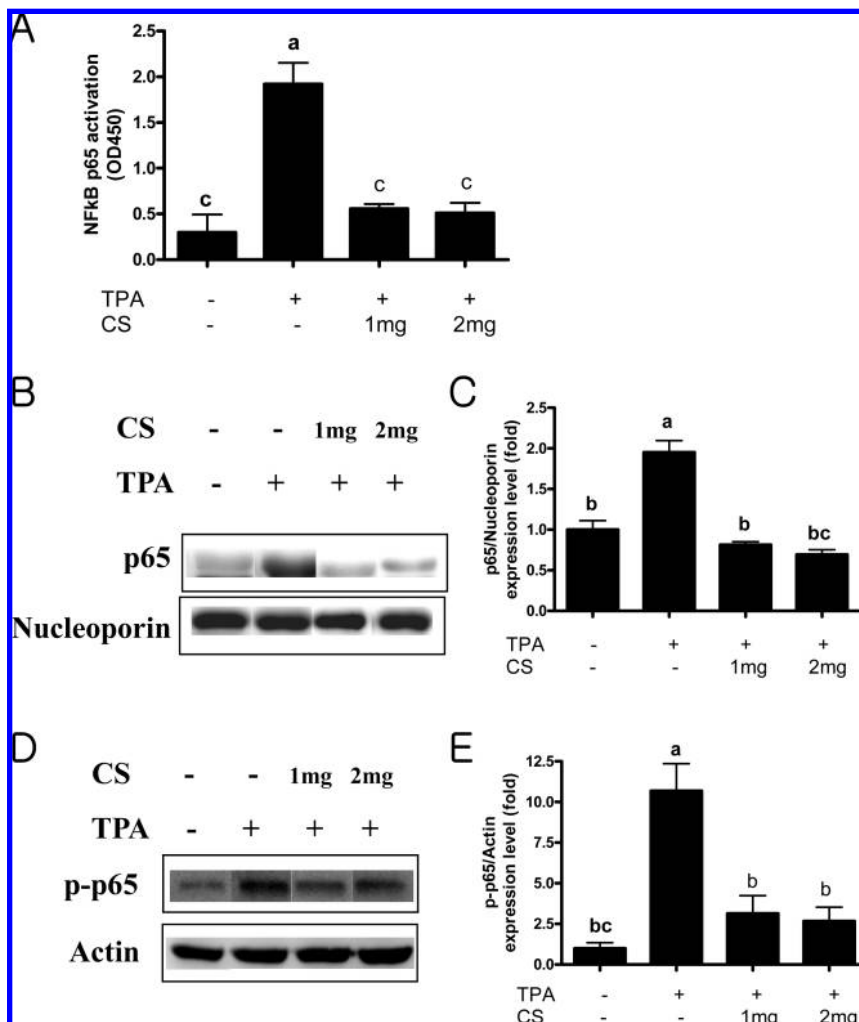


**Figure 3.** Inhibitory effects of CS on TPA-induced NF- $\kappa$ B activation in mouse skin. Mice were treated topically with TPA (200  $\mu$ L of 10 nmol of TPA dissolved in acetone) in the presence or absence of CS (1 or 2 mg). Control animals were treated with acetone only. (A) NF- $\kappa$ B p65 DNA binding activity; (B) Western blot analysis of p65 protein level in nuclear extract from mouse skin; (C) densitometric analysis of p65; (D) Western blot analysis of p-p65 protein level in mouse skin; (E) densitometric analysis of p-p65. Different letters (a–c) denote statistical difference ( $P < 0.05$ ). Each bar represents the mean  $\pm$  SE ( $n = 3$ ). CON, control; TPA, TPA-treated group; TPA + CS, TPA-treated mice in the presence of CS (1 or 2 mg).

then precipitated with 2 volumes of 95% ethanol for 2 h at 4  $^{\circ}$ C and centrifuged for 30 min at 8000 rpm. The precipitates were lyophilized and applied ( $\sim$ 250 mg) to a DEAE-Sepharose. A fast flow column (30  $\times$  5 cm) was equilibrated with 0.5 M sodium acetate buffer (pH 6.0). The column was developed by a linear gradient of 0–1.5 NaCl in the same buffer. The flow rate of the column was 5 mL/min, and fractions of  $\sim$ 25 mL were collected and assayed by metachromasia using 1,9-dimethylmethylene blue and by carbazole reaction for hexouronic acid. The positive fractions were pooled, dialyzed against distilled water, and lyophilized. The samples were reapplied to a newly packed DEAE-Sepharose. Again, the sample was repurified by the fast flow column as described above. The fractions of this second column containing GAGs were pooled, dialyzed against distilled water, and lyophilized (purity was 92.4%).

In addition, the purified GAGs were characterized with HPLC. Briefly, GAGs were treated with chondroitin ABC and/or AC lyase, and the digestive products were analyzed by HPLC on a Supelco 4.5 mm  $\times$  25 cm Spherisorb SAX column (Sigma-Aldrich), using a linear gradient of 0–1.0 M aqueous NaCl (pH 3.5) at a flow rate of 0.3 mL/min. Please note that chondroitin AC lyase cleaves only at glucuronate-containing disaccharides, that is, chondroitin sulfate; chondroitin B lyase cleaves only at iduronate-containing disaccharides, that is, dermatan sulfate, whereas chondroitin ABC lyase cleaves at either. With the aid of chondroitin AC and ABC lyase, therefore, classification of GAGs can be achieved efficiently. The

elution of the disaccharide was followed by absorbance at 232 nm, and they were identified by comparison with the elution positions of known disaccharide standards.

**Animal Treatment.** Female 5-week-old ICR mice purchased from Joongang Laboratory Animal (Seoul, Korea) were housed in the laboratory animal facility with temperature and relative humidity maintained at  $23 \pm 2$   $^{\circ}$ C and  $50 \pm 20\%$ , respectively, and were kept on a 12-h light/dark cycle. Mice were randomly divided into four groups (three mice per group) and CS (1 or 2 mg of CS dissolved in 200  $\mu$ L of distilled water) was topically applied to their shaven backs (about 200 mm<sup>2</sup>/site) after TPA treatment (10 nmol dissolved in acetone). Control animals were treated with acetone (200  $\mu$ L) alone. Four hours after treatment, mice were sacrificed, and the skin was collected for further analysis because topical application of TPA is known to induce COX-2 expression maximally at 4 h in mouse skin (8). Skin thickness was measured with digital thickness gauge (Mitutoyo Corp.). All methods used in this study were approved by the Animal Care and Use Committee at Seoul National University (SNU-061116-2).

**Western Blot Analysis.** Total cellular proteins were prepared from skin tissue as described in Hwang et al.'s method (23). After the protein concentration of homogenized lysates had been measured by using a Bradford kit (Bio-Rad, Hercules, CA), 30  $\mu$ g of protein was separated on SDS-PAGE and transferred to nitrocellulose membranes. The membranes were blocked for 1 h in TTBS containing 5% skim milk, and immunoblotting was done by incubating the membranes overnight

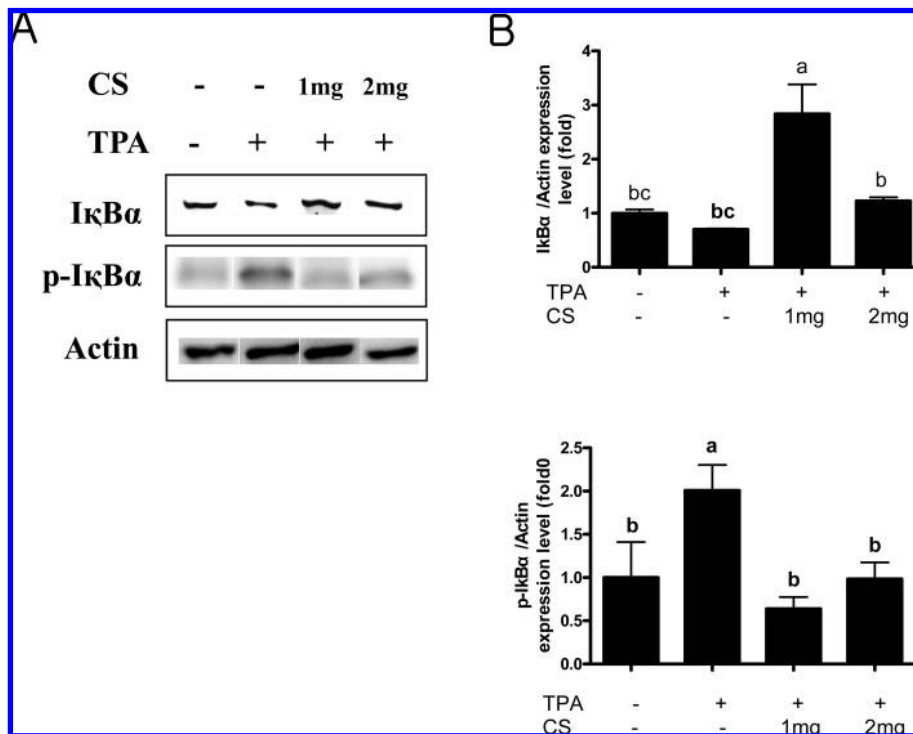


**Figure 4.** Inhibitory effects of CS on TPA-induced IκBα phosphorylation in mouse skin. Mice were treated topically with TPA (200 μL of 10 nmol of TPA dissolved in acetone) in the presence or absence of CS (1 or 2 mg). Control animals were treated with acetone only. (A) Western blot analysis of IκBα and p-IκBα expression; (B) bands of interest were further analyzed by densitometer. Different letters (a–c) denote statistical difference (*P* < 0.05). Each bar represents the mean ± SE (*n* = 3). CON, control; TPA, TPA-treated group; TPA + CS, TPA-treated mice in the presence of CS (1 or 2 mg).

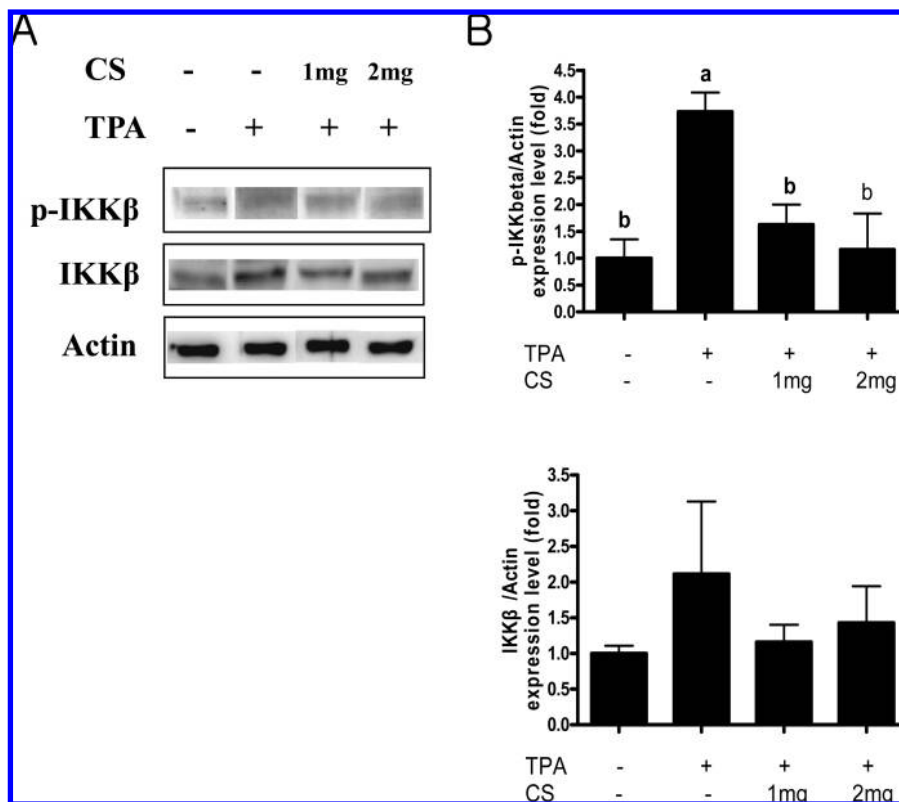


**Figure 5.** Inhibitory effects of CS on TPA-induced IKKβ phosphorylation in mouse skin. Mice were treated topically with TPA (200 μL of 10 nmol of TPA dissolved in acetone) in the presence or absence of CS (1 or 2 mg). Control animals were treated with acetone only. (A) Western blot analysis of IKKβ and p-IKKβ expression level in mouse skin; (B) bands of interests were further analyzed by densitometer. Different letters (a–c) denote statistical difference (*P* < 0.05). Each bar represents the mean ± SE (*n* = 3). CON, control; TPA, TPA-treated group; TPA + CS, TPA-treated mice in the presence of CS (1 or 2 mg).

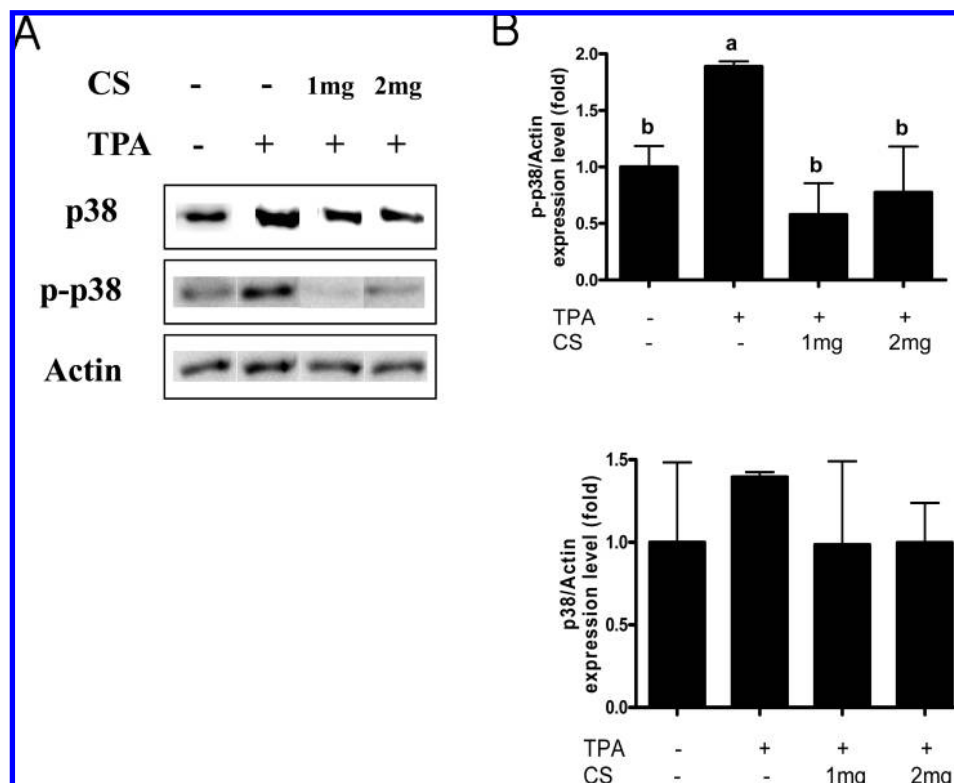


**Figure 6.** Inhibitory effects of CS on TPA-induced p38 phosphorylation in mouse skin. Mice were treated topically with TPA (200  $\mu$ L of 10 nmol of TPA dissolved in acetone) in the presence or absence of CS (1 or 2 mg). Control animals were treated with acetone only. (A) Western blot analysis of p38 and p-p38 expression level in mouse skin; (B) bands of interests were further analyzed by densitometer. Different letters (a, b) denote statistical difference ( $P < 0.05$ ). Each bar represents the mean  $\pm$  SE ( $n = 3$ ). CON, control; TPA, TPA-treated group; TPA + CS, TPA-treated mice in the presence of CS (1 mg or 2 mg).

with primary antibodies in 5% skim milk at 4  $^{\circ}$ C and then with secondary antibodies conjugated to horseradish peroxidase for 3 h at room temperature or overnight at 4  $^{\circ}$ C. After washing, the bands of interest were analyzed by luminescent image analyzer LAS-3000 (Fujifilm, Tokyo, Japan), and quantification of Western blot analysis was done by using Multi Gauge version 2.02 program (Fujifilm).

#### Nuclear Extract Separation and NF $\kappa$ B p65 DNA Binding Assay.

The nuclear fractions were prepared using a commercially available nuclear extract kit from Active Motif (Carlsbad, CA), and the nuclear extract was used to assess NF $\kappa$ B p65 DNA binding by using the ELISA-based TransAM NF- $\kappa$ B family transcription factor assay kit (Active Motif) following the manufacturer's instructions.

**Immunohistochemistry (IHC).** The skin tissues were fixed in 10% neutral buffered formalin, routinely processed, embedded in paraffin, and sectioned at 4  $\mu$ m. For IHC, the tissue sections were deparaffinized in xylene and rehydrated through alcohol gradients, then washed and incubated in 3% hydrogen peroxide (AppliChem, Darmstadt, Germany) for 30 min to quench endogenous peroxidase activity. After washing in PBS, the tissue sections were incubated with 5% BSA in PBS for 1 h at room temperature to block nonspecific binding. Primary antibodies were applied on tissue sections overnight at 4  $^{\circ}$ C. The following day, the tissue sections were washed and incubated with secondary HRP-conjugated antibodies (1:50) for 1 h at room temperature. After careful washing, tissue sections were counterstained with Mayer's Hematoxylin (Dako, Carpinteria, CA) and washed with xylene. Coverslips were mounted using Permount (Fisher, Pittsburgh, PA), and the slides were examined using a light microscope (Carl Zeiss, Thornwood, NY).

**Statistical Analysis.** All results are given as mean  $\pm$  SE, and statistical differences among treatment groups were analyzed by one-way analysis of variance and Duncan's multiple-range test using SAS statistical software package version 6.12 (SAS Institute, Cary, NC).

## RESULTS

**Characterization of Isolated GAGs.** CS can be divided into several kinds such as chondroitin sulfate A (CSA), chondroitin sulfate B (CSB), and chondroitin sulfate C (CSC), etc., in which CSA and CSC are the major ingredients in almost any animal species and tissue. CSA is the alternative name for chondroitin-6-sulfate, that is, chondroitin sulfate which is sulfated on the C6 position of the GlcNAc; however, CSC is sulfated at the 4-position (24). Our analytical results showed that CS isolated from ascidian tunic was a mixture of CSA and CSC (peak 2 for CSA and peak 3 for CSC; please see figure legends for detailed information; **Figure 1**), and peak area analysis in HPLC demonstrated that the ratio of CSA and CSC was 46:54 (see detailed calculation method in **Table 1**).

**Effects of CS on TPA-Induced Edema and Expression of COX-2 and VCAM-1 in Mouse Skin.** Because skin edema and inflammatory factors expression were evident from 3 h after TPA treatment in mouse skin (8, 25), potential effects of CS on TPA-induced skin edema and expression of inflammatory factors were measured. Our results showed that CS suppressed the TPA-induced edema (**Figure 2A,B**) and VCAM-1 expression (**Figure 2C**). Such suppression of VCAM-1 was clearly observed by densitometric analysis (**Figure 2D**). CS also suppressed TPA-induced COX-2 expression significantly, which was confirmed by IHC (**Figure 2E**) and by scoring COX-2 labeling index (**Figure 2F**) in skin of mice as well.

**TPA-Induced NF- $\kappa$ B Activation Was Negated by CS in the Mouse Skin.** The promoter region for COX-2 and VCAM-1 genes contains binding sites for various transcription factors including NF- $\kappa$ B (10). Our result clearly showed that both TPA-

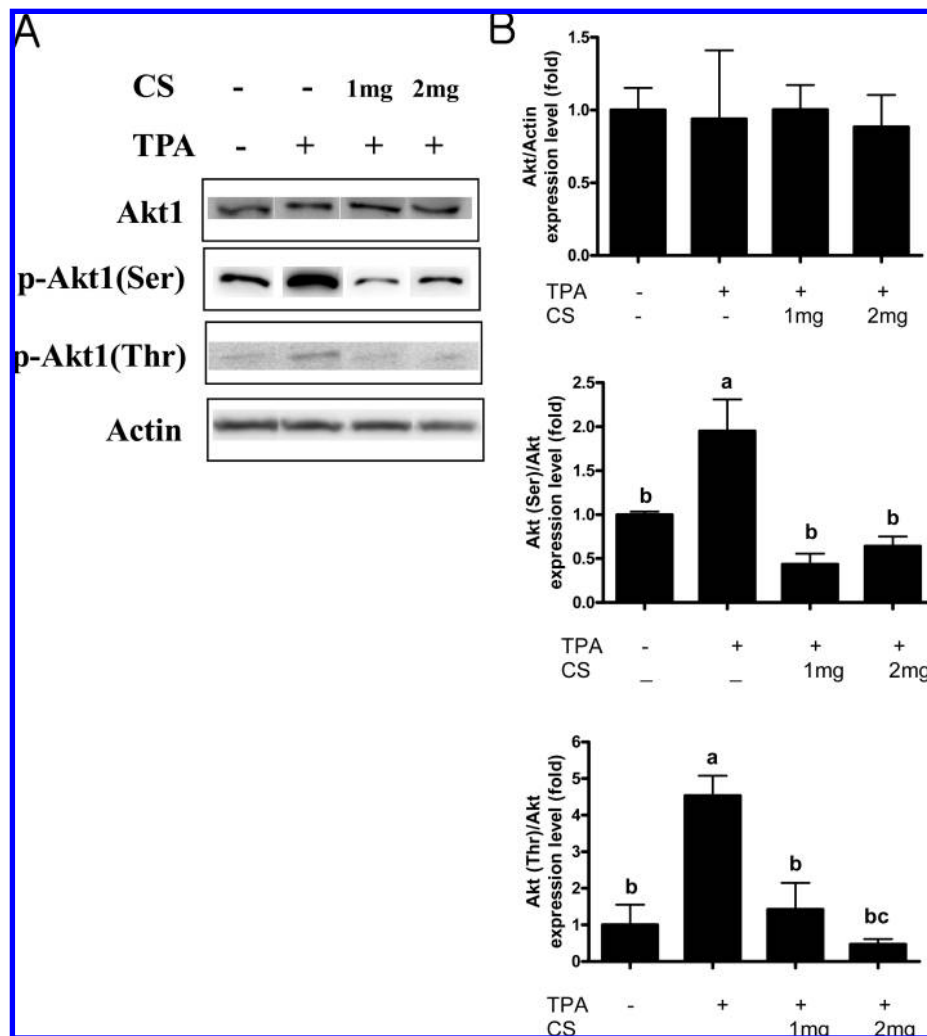


**Figure 7.** Inhibitory effects of CS on TPA-induced Akt phosphorylation in mouse skin. Mice were treated topically with TPA (200  $\mu$ L of 10 nmol of TPA dissolved in acetone) in the presence or absence of CS (1 or 2 mg). Control animals were treated with acetone only. (A) Western blot analysis of Akt and p-Akt expression level in mouse skin; (B) bands of interest were further analyzed by densitometer. Different letters (a–c) denote statistical difference ( $P < 0.05$ ). Each bar represents the mean  $\pm$  SE ( $n = 3$ ). CON, control; TPA, TPA-treated group; TPA + CS, TPA-treated mice in the presence of CS (1 or 2 mg).

induced NF- $\kappa$ B p65 protein nuclear translocation and DNA binding were significantly suppressed by CS treatment in mouse skin (Figures 3A–C). The transcriptional activation of NF- $\kappa$ B is regulated by the phosphorylation of its functionally active subunit p65 in its transcriptional activation domain (26). Our results also showed that CS suppressed TPA-induced phosphorylation of p65 in mouse skin (Figures 3D,E). Because nuclear translocation of NF- $\kappa$ B is dependent on the phosphorylation and subsequent degradation of I $\kappa$ B $\alpha$  (27), we also analyzed I $\kappa$ B $\alpha$  expression and its phosphorylation status. CS treatment significantly reduced TPA-stimulated phosphorylation of I $\kappa$ B $\alpha$  and subsequent degradation of I $\kappa$ B $\alpha$  (Figure 4).

**TPA-Induced Phosphorylation of I $\kappa$ B Kinase (IKK) Was Suppressed by CS in Mouse Skin.** The phosphorylation and degradation of I $\kappa$ B $\alpha$  are regulated by IKK, and the activation of IKK depends on the phosphorylation of its subunit IKK $\beta$  (27). As shown in Figure 5, topical application of TPA increased the phosphorylation of IKK $\beta$ , which was significantly inhibited by CS treatment.

**Effects of CS Treatment on TPA-Induced Phosphorylation of p38 in Mouse Skin.** MAPK is an important regulator of NF- $\kappa$ B and subsequent VCAM-1 and COX-2 expressions (8, 28). Thus, we examined the effect of CS on TPA-induced phospho-

rylation of p38 MAPK by Western blot analysis. As shown Figure 6, CS treatment significantly suppressed TPA-induced p38 phosphorylation.

**Effects of CS Treatment on TPA-Induced Phosphorylation of Akt in Mouse Skin.** Because Akt is known to regulate NF- $\kappa$ B activation (18) and COX-2 expression in mouse skin treated with TPA (23), we were interested in the potential effects of CS on Akt activation. Our result demonstrated that CS treatment significantly suppressed TPA-induced Akt phosphorylation both at Ser473 and at Thr308 (Figure 7A,B).

## DISCUSSION

There is a growing evidence of a supporting relationship between chronic inflammation and multistage carcinogenesis (3). Improper activation of inflammatory mediators has been shown to be associated with human cancers as well as inflammatory disorders (29). Therefore, a strategy to suppress the expression of pro-inflammatory factors may reduce the tumor incidence. In this regard, the present study showed anti-inflammatory effects of CS extracted from ascidian tunic on TPA-induced inflammation in mouse skin.

Recent study has indicated that COX-2 is involved in the causal relationship between inflammation and skin carcinogen-

esis as a key factor; thus, COX-2 would be a potential target for cancer prevention and treatment (1). Although several COX-2 inhibitors have been reported as anti-inflammatory agents, substantial warning against consumption of COX-2 is issued by regulatory agencies such as the U.S. FDA (23). VCAM-1 is another important inflammatory factor, and its role is also suggested in carcinogenesis, tumor angiogenesis, and metastasis (29). Therefore, development of safe VCAM-1 and COX-2 inhibitors retaining high efficacy is needed. This is why many scientists continue to search for safe anti-inflammatory chemicals from natural diet sources. The inhibition of TPA-induced COX-2 and VCAM-1 protein expressions by CS in mouse skin (Figure 2), thus, may provide a rational anti-inflammatory agent applicable to humans in the future. Moreover, information on the CS, demonstrating that CS isolated from ascidian tunic was a mixture of CSA and CSC (Figure 1) and that the ratio of CSA and CSC was 46:54 (Table 1), also supports the reproducibility of current work.

The activity of COX-2 and VCAM-1 is known to be regulated by the well-known transcription factor NF- $\kappa$ B, which plays an important role in inflammation-associated carcinogenesis (4). Treatment of mouse skin with CS negated the TPA-induced p65 activation, I $\kappa$ B $\alpha$  phosphorylation, and IKK $\beta$  phosphorylation, thus suggesting that CS suppressed COX-2 and VCAM-1 protein expressions through inactivation of NF- $\kappa$ B. Our finding is supported by a recent report that conjugated linoleic acid inhibited mouse skin carcinogenesis by blocking NF- $\kappa$ B translocation into the nucleus through suppression of phosphorylation and subsequent degradation of I $\kappa$ B $\alpha$  (23). Another line of evidence also suggests that p38 MAPK may regulate the transcriptional activity of NF- $\kappa$ B (16). In our study, treatment of CS suppressed the phosphorylation of p38 significantly (Figure 6), suggesting that CS ablated TPA-induced NF- $\kappa$ B activation through regulating upstream kinase p38, thus leading to reduction of COX-2 and VCAM-1 proteins.

Akt has been reported to regulate COX-2 and VCAM-1 expressions through the NF- $\kappa$ B/I $\kappa$ B pathway (18, 30). Many studies have shown that Akt regulated COX-2 protein expression in several different tissues such as skin and endometrial cancer (18, 23). Several lines of evidence demonstrated that Akt regulated COX-2 expression through I $\kappa$ B $\alpha$  phosphorylation (18, 23). This is consistent with our findings that TPA-induced Akt activation was suppressed by CS treatment (Figure 7). Taken together, CS appears to suppress TPA-induced COX-2 and VCAM-1 expressions partly through ablation of Akt activity.

In conclusion, CS inhibited TPA-induced NF- $\kappa$ B activation and subsequent COX-2 and VCAM-1 expression by blocking IKK $\beta$  and Akt/PKB signaling in mouse skin in vivo, thus suggesting that CS from ascidian tunic may be developed as an effective natural anti-inflammatory agent in the future.

## LITERATURE CITED

- Coussens, L. M.; Werb, Z. Inflammation and cancer. *Nature* **2002**, *420*, 860–867.
- Mareel, M.; Leroy, A. Clinical, cellular and molecular aspects of cancer invasion. *Physiol. Rev.* **2003**, *83*, 337–376.
- Arias, J. I.; Aller, M. A.; Arias, J. The use of inflammation by tumor cells. *Cancer* **2005**, *104*, 223–228.
- Aggarwal, B. B. Nuclear factor- $\kappa$ B: the enemy within. *Cancer Cell* **2004**, *6*, 203–208.
- Nam, N. Naturally occurring NF- $\kappa$ B inhibitors. *Mini Rev. Med. Chem.* **2006**, *6*, 945–951.
- Kundu, J. K.; Surh, Y. J. Breaking the relay in deregulated cellular signal transduction as a rationale for chemoprevention with anti-inflammatory phytochemicals. *Mutat. Res.* **2005**, *591*, 123–146.
- Kumar, A.; Takada, Y.; Boriek, A. M.; Aggarwal, B. B. Nuclear factor- $\kappa$ B: its role in health and disease. *J. Mol. Med.* **2004**, *82*, 434–448.
- Chun, K. S.; Keum, Y. S.; Han, S. S.; Song, Y. S.; Kim, S. H.; Surh, Y. J. Curcumin inhibits phorbol ester-induced expression of cyclooxygenase-2 in mouse skin through suppression of extracellular signal-regulated kinase activity and NF- $\kappa$ B activation. *Carcinogenesis* **2003**, *24*, 1515–1524.
- Osakabe, N.; Takano, H.; Sanbongi, C.; Yasuda, A.; Yanagisawa, R.; Inoue, K. I.; Yoshikawa, T. Anti-inflammatory and anti-allergic effect of rosmarinic acid (RA); inhibition of seasonal allergic rhinoconjunctivitis (SAR) and its mechanism. *Biofactors* **2004**, *21*, 127–131.
- Collins, T.; Read, M. A.; Neish, A. S.; Whitley, M. Z.; Thanos, D.; Maniatis, T. Transcriptional regulation of endothelial cell adhesion molecules: NF- $\kappa$ B and cytokine-inducible enhancers. *FASEB J.* **1995**, *9*, 899–909.
- Kim, Y.; Fischer, S. M. Transcriptional regulation of cyclooxygenase-2 in mouse skin carcinoma cells. Regulatory role of CCAAT/enhancer-binding proteins in the differential expression of cyclooxygenase-2 in normal and neoplastic tissues. *J. Biol. Chem.* **1998**, *273*, 27686–27694.
- Baldwin, A. S., Jr. The NF- $\kappa$ B and I $\kappa$ B proteins: new discoveries and insights. *Annu. Rev. Immunol.* **1996**, *14*, 649–683.
- Pahl, H. L. Activators and target genes of Rel/NF- $\kappa$ B transcription factors. *Oncogene* **1999**, *18*, 6853–6866.
- Greten, F. R.; Eckmann, L.; Greten, T. F.; Park, J. M.; Li, Z. W.; Egan, L. J.; Kagnoff, M. F.; Karin, M. IKK $\beta$  links inflammation and tumorigenesis in a mouse model of colitis-associated cancer. *Cell* **2004**, *118*, 285–296.
- Pikarsky, E.; Porat, R. M.; Stein, I.; Abramovitch, R.; Amit, S.; Kasev, S.; Gukovitch-Pyest, E.; Urieli-Shoval, S.; Galun, E.; Ben-Neriah, Y. NF- $\kappa$ B functions as a tumour promoter in inflammation-associated cancer. *Nature* **2004**, *431*, 461–466.
- Kim, S. O.; Kundu, J. K.; Shin, Y. K.; Park, J. H.; Cho, M. H.; Kim, T. Y.; Surh, Y. J. [6]-Gingerol inhibits COX-2 expression by blocking the activation of p38 MAP kinase and NF- $\kappa$ B in phorbol ester-stimulated mouse skin. *Oncogene* **2005**, *24*, 2558–2567.
- Kim, H. W.; Park, I. K.; Cho, C. S.; Lee, K. H., Jr.; Colburn, N. H.; Cho, M. H. Aerosol delivery of glucosylated polyethylenimine/phosphatase and tensin homologue deleted on chromosome 10 complex suppresses Akt downstream pathways in the lung of K-ras null mice. *Cancer Res.* **2004**, *64*, 7971–7976.
- St-Germain, M. E.; Gagnon, V.; Parent, S.; Asselin, E. Regulation of COX-2 protein expression by Akt in endometrial cancer cells is mediated through NF- $\kappa$ B/I $\kappa$ B pathway. *Mol. Cancer* **2004**, *3*, 7.
- Fioravanti, A.; Collodel, G. In vitro effects of chondroitin sulfate. *Adv. Pharmacol.* **2006**, *53*, 449–465.
- Legendre, F.; Baugé, M.; Roche, R.; Saurel, A. S.; Pujol, J. P. Chondroitin sulfate modulation of matrix and inflammatory gene expression in IL-1 $\beta$ -stimulated chondrocytes-study in hypoxic alginate bead cultures. *Osteoarthritis Cartilage* **2008**, *16*, 105–114.
- Campo, G. M.; Avenoso, A.; Campo, S.; D'Ascola, A.; Traina, P.; Calatroni, A. Chondroitin-4-sulphate inhibits NF- $\kappa$ B translocation and caspase activation in collagen-induced arthritis in mice. *Osteoarthritis Cartilage* **2008**, Epub ahead of print.
- Fuller, S. A.; Takahashi, M.; Hurrell, J. G. G. Preparation of monoclonal antibodies. In *Current Protocols in Molecular Biology*; Ausubel, F. M., Brent, R., Kingston, R. E., Moore, D. D., Seidman, J. G., Smith, J. A., Struhl, K., Eds.; Wiley: New York, 2007; pp 11.4.1–11.11.5.
- Hwang, D. M.; Kundu, J. K.; Shin, J. W.; Lee, J. C.; Lee, H. J.; Surh, Y. J. *cis*-9, *trans*-11 conjugate linoleic acid down regulates phorbol ester induced NF- $\kappa$ B activation and subsequent COX-2 expression in hairless mouse skin by targeting I $\kappa$ B kinase and PI3K-Akt. *Carcinogenesis* **2007**, *28*, 363–371.



- (24) Li, T.; Liu, S.; Liu, Z.; Hu, X. A sensitive and simple method for the determination of chondroitin sulfate A with crystal violet by resonance Rayleigh scattering technique. *Arch. Pharm. Chem. Life Sci.* **2005**, *338*, 427–432.
- (25) Murakawa, M.; Yamaoka, K.; Tanaka, Y.; Fukuda, Y. Involvement of tumor necrosis factor (TNF)- $\alpha$  in phorbol ester 12-*O*-tetradecanoylphorbol-13-acetate (TPA)-induced skin edema in mice. *Biochem. Pharmacol.* **2006**, *71*, 1331–1336.
- (26) Jiang, X.; Takahashi, N.; Ando, K.; Otsuka, T.; Tetsuka, T.; Okamoto, T. NF- $\kappa$ B p65 transactivation domain is involved in the NF- $\kappa$ B-inducing kinase pathway. *Biochem. Biophys. Res. Commun.* **2003**, *301*, 583–590.
- (27) Karin, M. How NF- $\kappa$ B is activated: the role of the I $\kappa$ B $\alpha$  kinase (IKK) complex. *Oncogene* **1999**, *18*, 6867–6874.
- (28) Lin, W. N.; Luo, S. F.; Lee, C. W.; Wang, C. C.; Wang, J. S.; Yang, C. M. Involvement of MAPKs and NF- $\kappa$ B in human tracheal smooth muscle cells. *Cell. Signal.* **2007**, *19*, 1258–1267.
- (29) Ding, Y. B.; Chen, G. Y.; Xia, J. G.; Zang, X. W.; Yang, H. Y.; Yang, L. Association of VCAM-1 overexpression with oncogenesis, tumor angiogenesis and metastasis of gastric carcinoma. *World J. Gastroenterol* **2003**, *9*, 1409–1414.
- (30) Tung, W. H.; Sun, C. C.; Hsieh, H. L.; Wang, S. W.; Horng, J. T.; Yang, C. M. EV71 induces VCAM-1 expression via PDGF receptor, PI3-K/Akt, p38MAPK, JNK and NF- $\kappa$ B in vascular smooth muscle cells. *Cell. Signal.* **2007**, *19*, 2127–2137.

---

Received for review May 21, 2008. Revised manuscript received July 31, 2008. Accepted August 19, 2008. This work was partially supported by grants from the KOSEF (M20702000006-08N0200-00610). M.-H.C. is supported by the Nano Systems Institute–National Core Research Center (NSI-NCRC) program of KOSEF. C.-X.X., H.J., Y.-S.C., and J.-Y.S. are also grateful for the award of the BK21 fellowship. K.-H.L. was supported by the 21C Frontier Functional Human Genome Project (FG03-0601-003-1-0-0) and the National Nuclear R&D Program from the Ministry of Science and Technology. G.R.B. was supported by National Cancer Institute Grant CA84573.

JF801578X